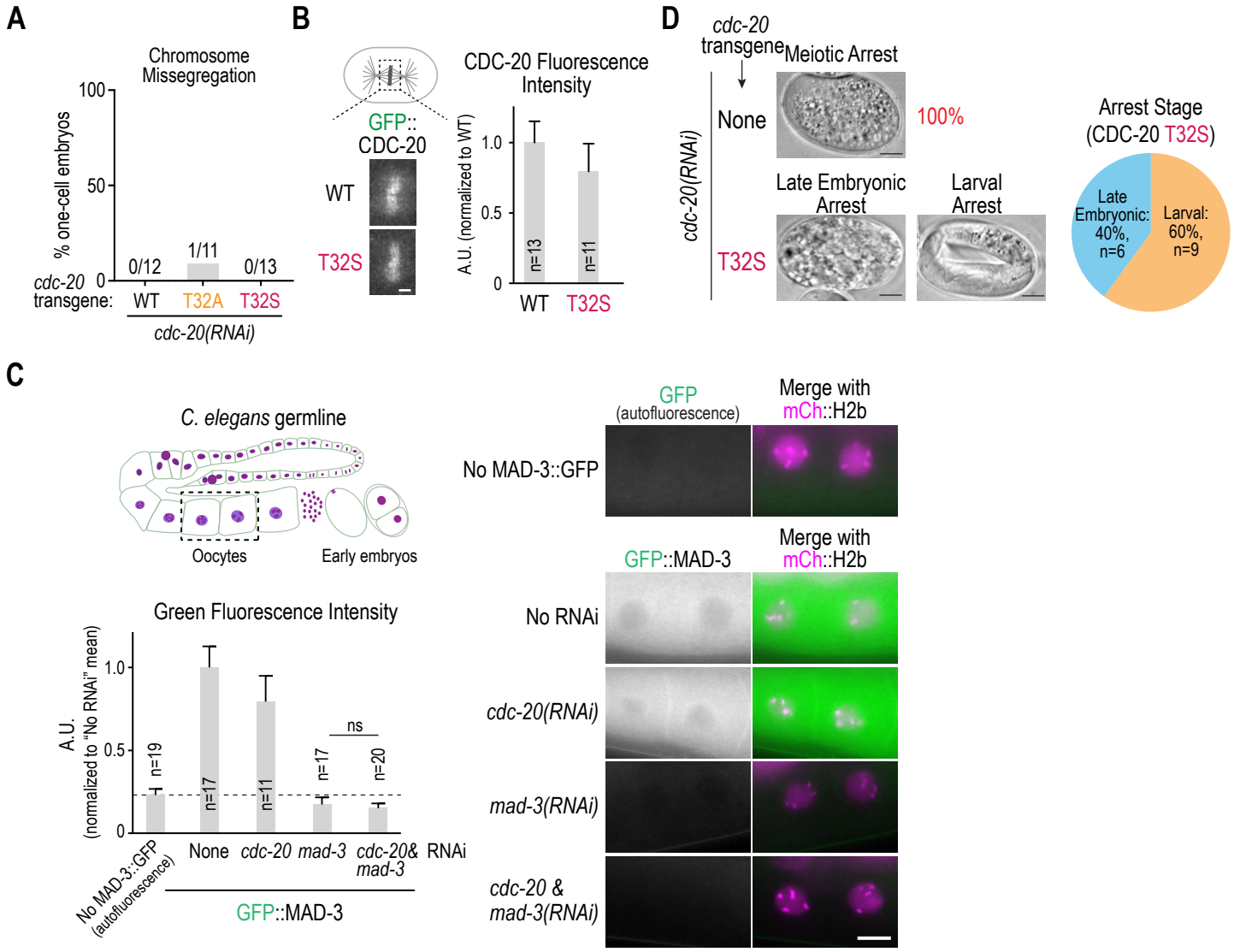
A
Chromosome Missegregation
% one-cell embryos
100
50
0
0/12
1/11
0/13
cdc-20 transgene:
WT
T32A
T32S
cdc-20(RNAi)
B
GFP:: CDC-20
WT
T32S
CDC-20 Fluorescence Intensity
A.U. (normalized to WT)
1.0
0.5
0
n=13
n=11
WT
T32S
D
cdc-20 transgene
Meiotic Arrest
cdc-20(RNAi)
None
100%
Late Embryonic Arrest
Larval Arrest
T32S
Arrest Stage (CDC-20 T32S)
Late Embryonic: 40%, n=6
Larval: 60%, n=9
C
C. elegans germline
Oocytes
Early embryos
Green Fluorescence Intensity
A.U. (normalized to "No RNAi" mean)
1.0
0.5
0
n=19
n=17
n=11
n=17
n=20
ns
No MAD-3::GFP (autofluorescence)
None
cdc-20
mad-3
cdc-20& mad-3
RNAi
GFP::MAD-3
GFP (autofluorescence)
Merge with mCh::H2b
No MAD-3::GFP
GFP::MAD-3
Merge with mCh::H2b
No RNAi
cdc-20(RNAi)
mad-3(RNAi)
cdc-20 & mad-3(RNAi)

Figure S1: Additional analysis of CDC-20 T32A and T32S mutants (related to Figure 1). **(A)** Chromosome missegregation in the indicated conditions. Missegregation was scored as visible lagging chromatin in anaphase (for an example image, see *Figure 2G*). No missegregation was observed for WT or T32S CDC-20; for T32A CDC-20, one of eleven imaged embryos exhibited mild lagging chromatin. **(B)** Localization analysis of GFP-fused WT and T32S CDC-20. *n* is number of embryos imaged per condition. Scale bar, 2 μm. **(C)** Assessment of the efficiency of MAD-3 depletion using an *in situ*-tagged GFP::MAD-3 strain. Oocytes preceding the spermatheca were imaged for the indicated conditions. A "No GFP::MAD-3" strain was used to measure autofluorescence in the green channel. Both *mad-3(RNAi)* alone and the *cdc-20&mad-3(RNAi)* mixture used for the experiment in *Figure 1E* were equally effective at reducing GFP::MAD-3 signal to the autofluorescence background. *n* is the number of oocytes imaged and analyzed. Scale bar, 10 μm. **(D)** Phenotypes of arrested/dead embryos and larvae observed with T32S CDC-20. Chart on the right quantifies the frequency of observed arrest states. When no transgene is present, CDC-20 depletion leads to meiotic arrest, which is shown on top. Scale bar, 10 μm. All error bars are the 95% confidence interval.

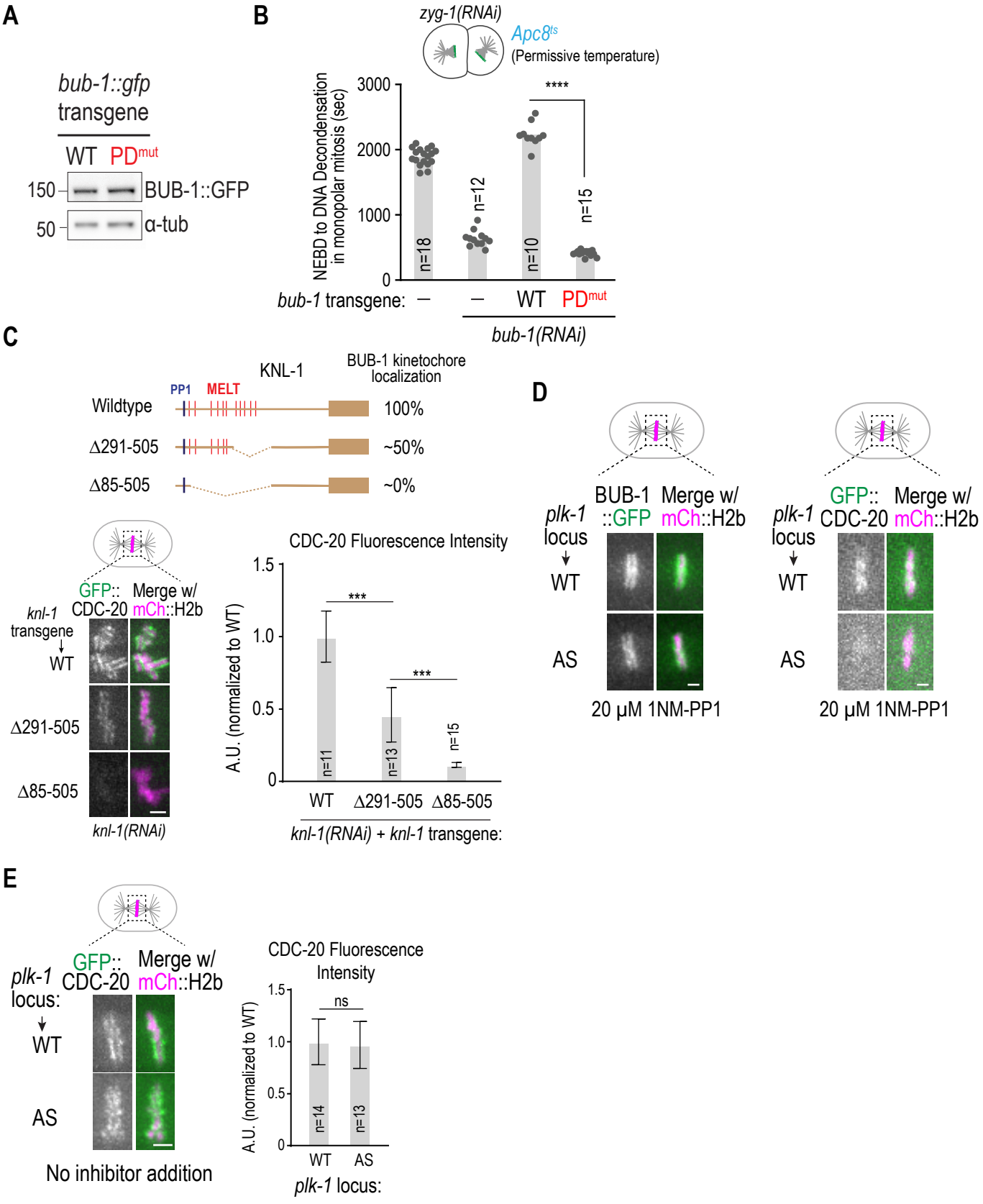
A
bub-1::gfp
transgene
WT PDmut
150
BUB-1::GFP
50
α-tub
B
zyg-1(RNAi)
Apc8ts
(Permissive temperature)
NEBD to DNA Decondensation in monopolar mitosis (sec)
3000
2000
1000
0
****
n=18
n=12
n=10
n=15
bub-1 transgene: – – WT PDmut
bub-1(RNAi)
C
KNL-1
BUB-1 kinetochore localization
PP1
MELT
Wildtype
100%
Δ291-505
~50%
Δ85-505
~0%
knl-1 transgene
WT
Δ291-505
Δ85-505
GFP:: CDC-20
Merge w/ mCh::H2b
knl-1(RNAi)
CDC-20 Fluorescence Intensity
A.U. (normalized to WT)
1.5
1.0
0.5
0
***
***
n=11
n=13
n=15
WT Δ291-505 Δ85-505
knl-1(RNAi) + knl-1 transgene:
D
plk-1 locus
WT
AS
BUB-1 ::GFP
Merge w/ mCh::H2b
20 μM 1NM-PP1
plk-1 locus
WT
AS
GFP:: CDC-20
Merge w/ mCh::H2b
20 μM 1NM-PP1
E
plk-1 locus:
WT
AS
GFP:: CDC-20
Merge w/ mCh::H2b
No inhibitor addition
CDC-20 Fluorescence Intensity
A.U. (normalized to WT)
1.5
1.0
0.5
0
ns
n=14
n=13
WT AS
plk-1 locus:

Figure S2: Additional analysis of PLK-1 docking mutant BUB-1 and of PLK-1 kinase activity inhibition (related to Figures 2 & 3).

(A) Immunoblot of WT and PD^{mut} BUB-1::GFP expressed from single-copy transgene insertions. PD^{mut} BUB-1 is expressed at similar level to WT BUB-1. α-tubulin serves as a loading control. **(B)** Analysis of spindle checkpoint signaling in PD^{mut} BUB-1. Spindle checkpoint signaling at unattached kinetochores was analyzed using monopolar spindle formation in 2-cell embryos induced by depletion of ZYG-1, which is essential for centriole duplication; $Apc8^{ts}$ at the permissive temperature was used to enhance sensitivity of the checkpoint assay [S1]. Time from NEBD to chromosome decondensation was monitored from timelapse movies of GFP::H2b. Depletion of BUB-1 abolishes checkpoint signaling and is rescued by expression of RNAi-resistant transgene-encoded WT BUB-1. By contrast, PD^{mut} BUB-1 failed to rescue, which is consistent with the inability of CDC-20 to localize to kinetochores in this mutant. *n* is the number of embryos quantified. **(C)** CDC-20 localization analysis in KNL-1 mutants that partially or completely eliminate BUB-1 kinetochore localization. Repetitive MELT motifs in the KNL-1 N-terminus recruit BUB-1; the Δ291-505 mutant reduces BUB-1 levels by ~50%, whereas the Δ85-505 mutant eliminates BUB-1 localization[S2]. CDC-20 localization appears to parallel that of BUB-1. *n* is the number of embryos imaged and quantified**.** **(D)** Additional examples of BUB-1::GFP and GFP::CDC-20 localization following temporally-controlled PLK-1 inhibition. Scale bar, 2 μm. **(E)** Images and quantification of CDC-20 localization in embryos expressing either WT or AS PLK-1. Embryos were imaged without permeabilization and inhibitor addition. There is no significant change in CDC-20 kinetochore localization between the two conditions. *n* is the number of embryos quantified.Scale bar, 2 μm. All error bars are the 95% confidence interval. p-values are from unpaired t-tests; ****: $p<0.0001$; ***: $p<0.001$; ns: not significant.

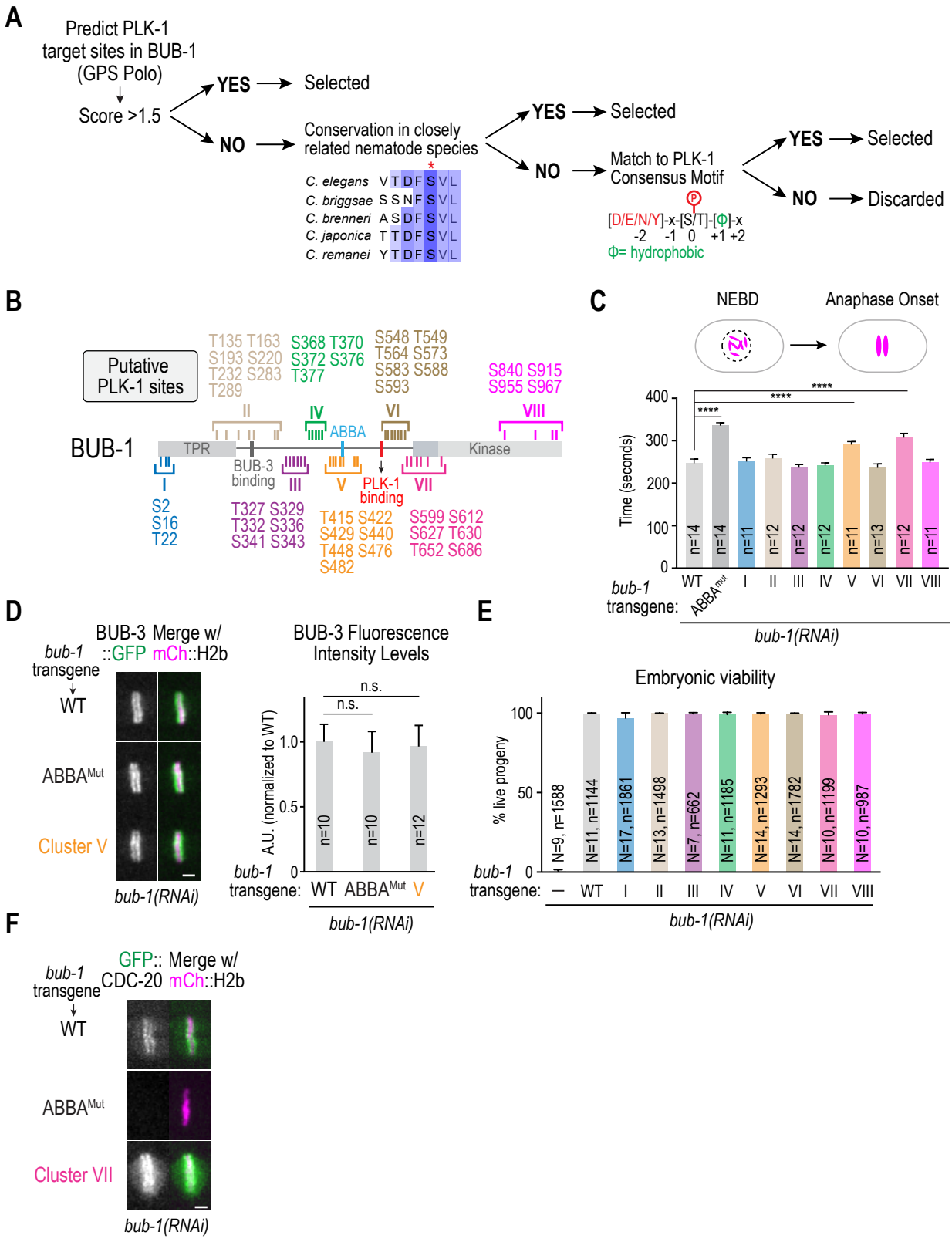
A
Predict PLK-1 target sites in BUB-1 (GPS Polo)
Score >1.5
YES
Selected
NO
Conservation in closely related nematode species
C. elegans V T D F S V L
C. briggsae S S N F S V L
C. brenneri A S D F S V L
C. japonica T T D F S V L
C. remanei Y T D F S V L
YES
Selected
NO
Match to PLK-1 Consensus Motif
[D/E/N/Y]-x-[S/T]-[Φ]-x
-2 -1 0 +1 +2
Φ= hydrophobic
YES
Selected
NO
Discarded
B
Putative PLK-1 sites
T135 T163 S193 S220 T232 S283 T289
S368 T370 S372 S376 T377
S548 T549 T564 S573 S583 S588 S593
S840 S915 S955 S967
BUB-1
TPR
ABBA
Kinase
BUB-3 binding
PLK-1 binding
S2 S16 T22
T327 S329 T332 S336 S341 S343
T415 S422 S429 S440 T448 S476 S482
S599 S612 S627 T630 T652 S686
C
NEBD
Anaphase Onset
Time (seconds)
bub-1 transgene:
WT
ABBA mut
bub-1(RNAi)
D
BUB-3 ::GFP
Merge w/ mCh::H2b
bub-1 transgene
WT
ABBA Mut
Cluster V
bub-1(RNAi)
BUB-3 Fluorescence Intensity Levels
A.U. (normalized to WT)
n.s.
bub-1 transgene:
WT ABBA Mut V
bub-1(RNAi)
E
Embryonic viability
% live progeny
bub-1 transgene:
WT
bub-1(RNAi)
F
GFP:: CDC-20
Merge w/ mCh::H2b
bub-1 transgene
WT
ABBA Mut
Cluster VII
bub-1(RNAi)

Figure S3: Selection and analysis of putative PLK-1 sites in BUB-1 (related to Figure 3).

(A) Schematic of approach used to select 45 putative PLK-1 target sites in BUB-1. **(B)** List of sites in the 8 clusters that were mutated to alanine. **(C)** NEBD-anaphase onset interval in the cluster mutants. **(D)** Analysis of BUB-3::GFP localization in the indicated conditions. (*left*) Example images of BUB-3::GFP localization; (*right*) quantification of BUB-3::GFP signal on aligned chromosomes. BUB-3 requires BUB-1 for its kinetochore localization; normal BUB-3 localization in the Cluster V mutant indicates that the 7 sites mutated do not affect BUB-1 kinetochore localization. **(E)** Embryonic viability analysis for the indicated conditions. *N* is number of worms analyzed and *n* is the total number of embryos scored. **(F)** Image of CDC-20 hyper-localization in the Cluster VII mutant. For quantification, see *Figure 3F*. *n* is the number of embryos quantified. Scale bar, 2 μm. All error bars are the 95% confidence interval. p-values are from unpaired t-tests; ****: $p<0.0001$; n.s.= not significant.

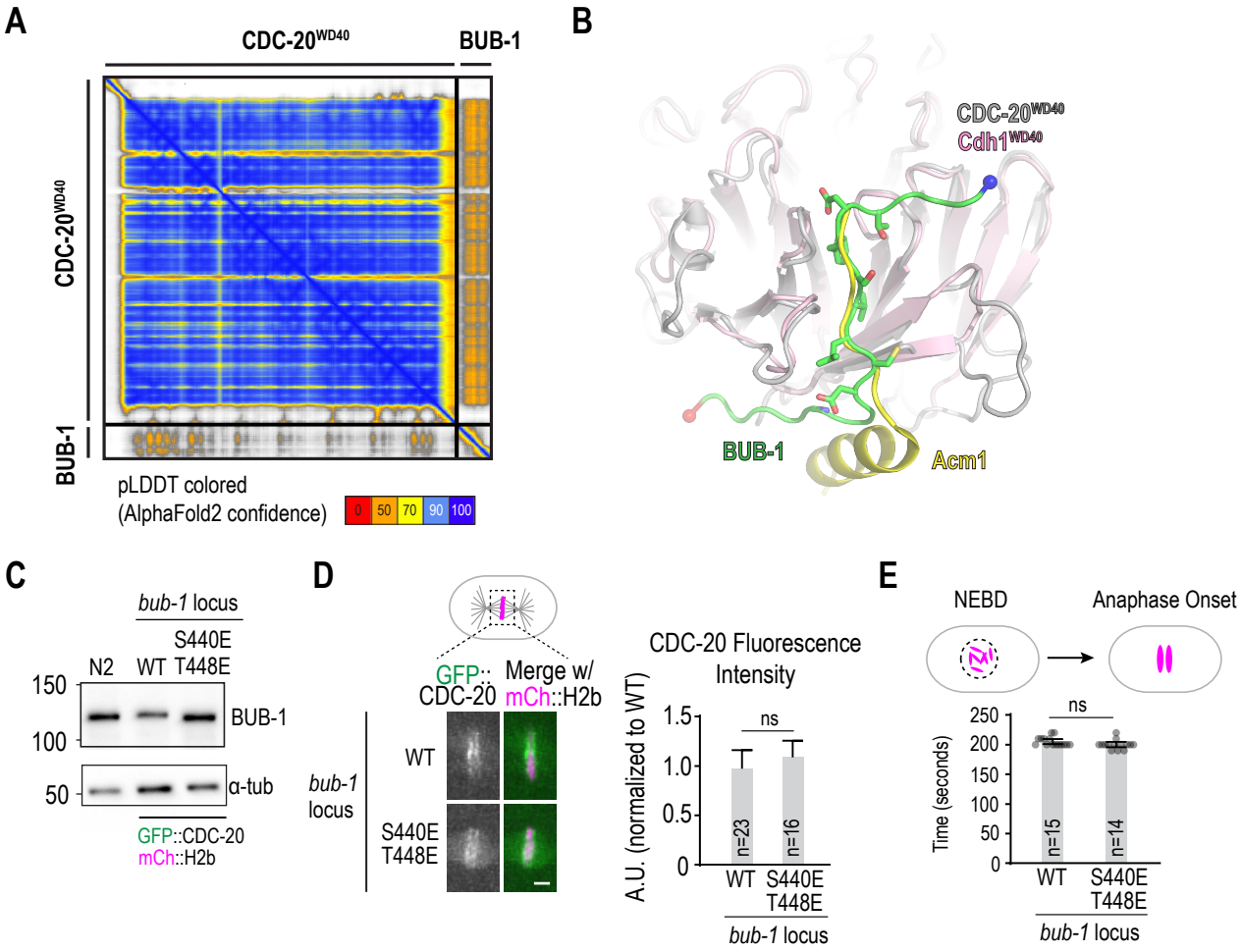
A
CDC-20WD40
BUB-1
CDC-20WD40
BUB-1
pLDDT colored
(AlphaFold2 confidence)
0
50
70
90
100
B
CDC-20WD40
Cdh1WD40
BUB-1
Acm1
C
bub-1 locus
S440E
N2
WT
T448E
150
100
50
BUB-1
α-tub
GFP::CDC-20
mCh::H2b
D
GFP::
CDC-20
Merge w/
mCh::H2b
bub-1
locus
WT
S440E
T448E
CDC-20 Fluorescence
Intensity
A.U. (normalized to WT)
1.5
1.0
0.5
0
ns
n=23
n=16
WT
S440E
T448E
bub-1 locus
E
NEBD
Anaphase Onset
Time (seconds)
250
200
150
100
50
0
ns
n=15
n=14
WT
S440E
T448E
bub-1 locus

Figure S4: Alphafold model of CDC-20 WD40 domain interaction with the BUB-1 ABBA region and characterization of phosphomimetic BUB-1 mutants (related to Figure 4).

(A) Predicted alignment error (PAE) plot of the confidence of the AlphaFold2 model shown in *Figure 4E*. **(B)** Structural superposition of *C. elegans* CDC-20 WD40 domain::BUB-1 ABBA motif model with the structure of *S. cerevisiae* Cdh1::Acm1 A motif (PDB ID 4BH6). The root mean square deviation for the superposition of S. cerevisiae Cdh1 WD40 with *C. elegans* CDC-20 WD40 is 0.76 Å for 212 Cα atoms. **(C)** Immunoblot of the indicated conditions. The WT and S440E;T448E lanes are from the strain expressing GFP::CDC-20 and mCh::H2b in which the CRISPR/Cas9 editing to introduce the phosphomimetic mutations was performed. The N2 lane is from the wildtype N2 strain. **(D)** Images and quantification of CDC-20 localization for the indicated conditions. The phosphomimetic substitutions S440E;T448E did not perturb CDC-20 kinetochore localization. Data for wildtype is same as shown in *Figure 4B*. *n* is the number of embryos quantified. Scale bar, 2 µm. **(E)** NEBD-anaphase onset interval comparing WT and phosphomimetic S440E,T448E BUB-1. No significant change in mitotic duration is observed with the phosphomimetic mutant. Data for wildtype is same as shown in *Figure 4C*. *n* is the number of embryos quantified. p-values are from unpaired t-tests; n.s.= not significant.

Residue #	Sequence	Score	Score > 1.5	Consensus	Conserved ? (S or T)
2	******MSHIRVAFA	1.529	YES	No	YES
16	APLDTNPSTCGLETF	1.051	No	YES	YES
22	PSTCGLETFATQIET	0.71	No	YES	No
135	LSERIEMTAIESGFR	2.395	YES	YES	No
163	MFTRPDETMDLFRFN	3.062	YES	YES	YES
193	HNVPINNSGKAAFGP	1.732	YES	YES	No
220	RPNYHGISIEEFRFA	1.583	YES	No	YES
232	RFAKWKDTFGEDVDD	1.094	No	YES	No
283	NPRRRHLSPVSEKTV	1.728	YES	No	No
289	LSPVSEKTVDDEEEK	3.243	YES	YES	No
327	ENPPATVTLSSDTKS	1.891	YES	No	YES
329	PPATVTLSSDTKSAS	1.663	YES	No	YES
332	TVTLSSDTKSASEKD	1.616	YES	No	YES
336	SSDTKSASEKDVSDS	2.047	YES	No	No
341	SASEKDVSDSDDADD	4.562	YES	YES	YES
343	SEKDVSDSDDADDDE	2.018	YES	No	No
368	DGNPPDRSTSISSNY	3.134	YES	YES	No
370	NPPDRSTSISSNYST	3.457	YES	No	No
372	PDRSTSISSNYSTAS	1.594	YES	No	YES
376	TSISSNYSTASARTS	2.572	YES	YES	YES
377	SISSNYSTASARTSK	0.569	No	YES	YES
415	VHLASEKTMVLGDDS	2.681	YES	YES	YES
422	TMVLGDDSVFVPERS	4.355	YES	YES	No
429	SVFVPERSLATTQIV	2.246	YES	YES	No
440	TQIVTDFSVLCDPDP	3.337	YES	YES	YES
448	VLCDPDPTMTITQER	2.688	YES	YES	YES
476	EAAEPEESQKVEESE	3.293	YES	YES	No
482	ESQKVEESEVQPEIV	4.536	YES	YES	No
548	FGNKEEESTHEQEAP	2.645	YES	YES	No
549	GNKEEESTHEQEAPV	1.634	YES	YES	No
564	FVAPTSSTFSKLTRR	2.775	YES	YES	No
573	SKLTRRKSLAANQAV	2.587	YES	No	YES
583	ANQAVQPSVTESSKP	4.768	YES	No	No
588	QPSVTESSKPERSDP	3.757	YES	YES	No
593	ESSKPERSDPKDSSI	3.051	YES	YES	No
599	RSDPKDSSIDCLTAN	4.931	YES	YES	YES
612	ANLGRRLSIGADEIP	1.837	YES	No	YES
627	NLTENNESEITGCKI	2.833	YES	YES	No

630	ENNESEI**T**GCKIRRR	1.446	No	YES	YES
652	DINPWDE**T**LRKKLMC	1.837	YES	YES	No
686	ALRDCEV**S**GEKLHIQ	2.217	YES	YES	No
840	DALMSND**S**FVIKIID	2.163	YES	YES	No
915	GASVGDY**S**LNVDIKR	3.822	YES	YES	No
955	DWNILIK**S**FSEIWNE	1.659	YES	YES	No
967	WNEKFEA**S**GWRQAV S	2.014	YES	YES	No

Table S1: List of sites mutated in clustered mutagenesis screen (related to Figure 3D-F)

Supplemental References

S1. Kim, T., Lara-Gonzalez, P., Prevo, B., Meitinger, F., Cheerambathur, D.K., Oegema, K., and Desai, A. (2017). Kinetochores accelerate or delay APC/C activation by directing Cdc20 to opposing fates. Genes Dev *31*, 1089-1094. 10.1101/gad.302067.117.

S2. Moyle, M.W., Kim, T., Hattersley, N., Espeut, J., Cheerambathur, D.K., Oegema, K., and Desai, A. (2014). A Bub1-Mad1 interaction targets the Mad1-Mad2 complex to unattached kinetochores to initiate the spindle checkpoint. J Cell Biol *204*, 647-657. 10.1083/jcb.201311015.